General and Comparative Endocrinology 296 (2020) 113538

Contents lists available at ScienceDirect

General and Comparative Endocrinology

journal homepage: www.elsevier.com/locate/ygcen

Research paper

Epigenetic regulation of gonadal and brain aromatase expression in a cichlid fish with environmental sex determination

Rose M.H. Driscoll[a,b], Josh J. Faber-Hammond[a], Cynthia F. O'Rourke[a], Peter L. Hurd[c,d], Suzy C.P. Renn[a,*]

[a] Department of Biology, Reed College, Portland, OR, USA
[b] Department of Biology, University of Rochester, Rochester, NY, USA
[c] Neuroscience and Mental Health Institute, University of Alberta, Edmonton, AB, Canada
[d] Department of Psychology, University of Alberta, Edmonton, AB, Canada

ARTICLE INFO

Keywords:
Aromatase
Environmental sex determination
Epigenetics
Kribensis
Methylation
Pelvicachromis pulcher

ABSTRACT

A fit animal must develop testes or ovaries, with brain and physiology to match. In species with alternative male morphs this coordination of development across tissues operates within sexes as well as between. For *Pelvicachromis pulcher*, an African cichlid in which early pH exposure influences both sex and alternative male morph, we sequence both copies of aromatase (cyp19a1), a key gene for sex determination. We analyze gene expression and epigenetic state, comparing gonad and brain tissue from females, alternative male morphs, and fry. Relative to brain, we find elevated expression of the A-copy in the ovaries but not testes. Methylation analysis suggests strong epigenetic regulation, with one region specifying sex and another specifying tissue. We find elevated brain expression of the B-copy with no sex or male morph differences. B-copy methylation follows that of the A-copy rather than corresponding to B-copy expression. In 30-day old fry, we see elevated B-copy expression in the head, but we do not see the expected elevated A-copy expression in the trunk that would reflect ovarian development. Interestingly, the A-copy epialleles that distinguish ovaries from testes are among the most explanatory patterns for variation among fry, suggesting epigenetic marking of sex prior to differentiation and thus laying the groundwork for mechanistic studies of epigenetic regulation of sex and morph differentiation.

1. Introduction

The relatively consistent and taxonomically pervasive outcome of differentiating into either a male (sperm-producing) or female (egg-producing) form is determined by a wildly diverse set of mechanisms across different animal species. Sex determination systems range from varieties of genetic sex determination (GSD) systems including XY or ZW chromosomal systems, polygenic sex determination systems, haplodiploidy, and paternal genome elimination, to environmental sex determination (ESD) systems. While sex determination is relatively static in some taxa, such as mammals and birds, in other lineages, such as teleost fish, even related species exhibit a diversity of sex determination systems and a diversity of master sex determiner genes. As an example of this rapid evolution, in the family Cichlidae alone, environmental influences of temperature and pH exist alongside striking diversity of genetic factors including B-chromosome, XY and ZW heterogametic sex chromosome systems as well as complex polyfactorial systems (e.g. Ser et al., 2010; Baroiller et al., 2009a; Yoshida et al 2011).

Downstream of this diversity in sex determination mechanisms lies a more conserved gene network governing sexual differentiation (Herpin and Schartl, 2015; Valenzuela et al., 2013). These ancestral and conserved genes connect the master sex determiner with the start of sexual differentiation pathways, and consistently show sexually differentiated expression early in gonadal development (Heule et al., 2014b; Kikuchi and Hamaguchi, 2013; Piferrer and Guiguen, 2008; Place and Lance, 2004; Valenzuela et al., 2013). In species exhibiting ESD, environmental factors likely act either at or upstream of the conserved set of downstream genes. One of these downstream genes in particular, the cyp19a1 gene, has been consistently associated with ESD mechanisms in a wide range of taxa including alligators, turtles, and fishes (Anastasiadi et al., 2018; Baroiller et al., 2009b; Matsumoto et al., 2013; Navarro-Martin et al., 2011; Parrott et al., 2014; Shen and Wang, 2014).

The cyp19a1 gene codes for an aromatase, the enzyme that converts androgens to estrogens. Estrogens such as estradiol are an essential

* Corresponding author.
E-mail address: renns@reed.edu (S.C.P. Renn).

https://doi.org/10.1016/j.ygcen.2020.113538
Received 10 January 2020; Received in revised form 11 March 2020; Accepted 14 May 2020
Available online 23 June 2020
0016-6480/

factor for ovarian differentiation throughout the vertebrate clade (Callard et al., 2001), from fish (Cutting et al., 2013; Li et al., 2009) to birds (Smith et al., 1997) and marsupials (Devlin and Nagahama, 2002; Coveney et al., 2001), with placental mammals deviating in timing and sensitivity (Yao, 2005). The cyp19a1 gene shows sexually dimorphic, female-biased expression early in sex determination in a highly conserved manner across vertebrates, putting regulation of this gene at the crux of primary sex determination and gonadal differentiation (Diotel et al., 2010; Lance, 2009; Valenzuela et al., 2013) though post-transcriptional regulation may also be involved. In teleosts, the absence of aromatase expression allows more testosterone to be converted to 11-hydroxy-oxygenated androgens and ultimately to the main fish androgen, 11-ketotestosterone (11-KT), blocking feminization and leading to testicular development.

Aromatase also plays a critical role in the sexual differentiation of the brain. The classic organizational/aromatization model of brain masculinization, in which a surge of testicular testosterone is aromatized to estradiol in the brain where estrogen receptor mediated processes permanently masculinize neural circuitry, is well founded in both birds and mammals (Balthazart et al., 2011; Maclusky and Naftolin, 1981; McCarthy et al., 2009; Naftolin et al., 1975; Nugent and McCarthy, 2011). Teleost fish, on the other hand, do not seem to have such a permanent organizational-activational masculinization of the brain. Rather, there is a life-long and reversible process of aromatase-driven maintenance of masculinization (Le Page et al., 2010) accompanied by brain aromatase levels orders of magnitude higher, in both sexes, than seen in mammals (Callard et al., 1990; Callard et al., 2001; González and Piferrer, 2002, 2003 Diotel et al., 2010; Pasmanik and Callard, 1985).

Most vertebrates have one aromatase gene (cyp19a1) with multiple tissue-specific promoters (Bulun et al., 2003; Golovine et al., 2003). Teleosts have two aromatase genes (cyp19a1A and cyp19a1B) resulting from an ancestral whole-genome duplication (Chiang et al., 2001; Taylor et al., 2003; Tchoudakova and Callard, 1998). These two aromatase gene copies have evolved largely separate roles; the A-copy, cyp19a1A, is expressed in the gonads and the B-copy, cyp19a1B, mainly in the brain but also in other tissues in most species (Blazquez and Piferrer, 2004; Callard et al., 2001; Cao et al., 2012; Chang et al., 2005; Trant et al., 2001). The East African cichlid radiation is a known exception to this rule (Böhne et al., 2013), but most cichlids follow this conventional pattern (Chang et al., 2005). In general, ovaries show higher A-copy expression than testes. However, there is little consistency within teleosts in the onset of this sex difference; zebrafish *Danio rerio* show an increase at the time of sexual differentiation, while medaka *Oryzias latipes*, European sea bass *Dicentrarchus labrax,* and Japanese flounder *Paralichthys olivaceus* show it after (Kitano et al., 1999; Navarro-Martin et al., 2011; Siegfried, 2010; Socorro et al., 2007). Nile tilapia *Oreochromis niloticus* (D'Cotta et al., 2001; Siegfried, 2010) and Atlantic halibut *Hippoglossus hippoglossus* show increased expression in females or female-biasing conditions (reviewed in: Shen and Wang, 2014) as early as 5 days post fertilization (Ijiri et al., 2008; Kobayashi et al., 2003), well before gonadal differentiation.

Likewise, there is no consistent sex bias for brain aromatase expression during development. Strongly bimodal expression in whole zebrafish fry is not associated with fry sex (Kallivretaki et al., 2007). Initial studies (Kwon et al., 2001) found a non-significant body-wide trend for higher B-copy expression in XX than XY Nile tilapia but later studies found no sex difference in whole brain samples during development (Chang et al., 2005; Sudhakumari et al., 2005). Medaka have inconsistently shown female-biased B-copy expression in brains during early development (Patil and Gunasekera, 2008) (but see: Okubo et al., 2011). Similarly, European sea bass inconsistently show sex differences in brain aromatase (but see: Blazquez et al., 2008). These diverse and conflicting results suggest species-specific patterns and heterogeneity across brain regions.

Epigenetic modifications such as DNA methylation and chromatin structure are thought to be central to the ESD mechanism through which early life environment influences sex (Gorelick, 2003; Piferrer, 2013). A wide range of species with temperature sex determination (TSD) show precisely such an effect in the cyp19a1 promoter (Piferrer, 2013), with higher methylation in testes than ovaries. Furthermore, male-biasing temperatures lead to increased methylation of the A-copy promoter within sexes for several fish species including European sea bass (Navarro-Martin et al., 2011), Nile tilapia (Wang et al., 2017) and mangrove killifish *Kryptolebias marmoratus* (Ellison et al., 2015). The same patterns are seen under ESD for species with only one copy of cyp19a1: male-producing temperatures result in higher cyp19a1 promoter methylation and decreased gonadal aromatase expression, and female-producing temperatures result in lower cyp19a1 methylation and increased in aromatase expression, in the American alligator *Alligator mississippiensis* (Parrott et al., 2014), Reeves' turtle *Mauremys reevesii* (Ru et al., 2017), and the red-eared slider turtle *Trachemys scripta* (Ramsey et al., 2007). In red-eared slider turtles, the brain initiates sexual differentiation and is sensitive to temperature effects prior to gonadal differentiation (Crews et al., 1996; Czerwinski et al., 2016). Exposure to masculinizing (high) temperatures also increases brain aromatase expression in the Mozambique tilapia *Oreochromis mossambicus* (Tsai et al., 2003). The degree to which within-sex variation in methylation impacts phenotypic variation is unknown, but exposure to sex-biasing temperatures also produces within-sex effects on sexual and territorial behaviors in the leopard gecko *Eublepharis macularius* (Flores et al., 1994; Rhen and Crews, 1999; Tsai et al., 2003).

Here we examine the epigenetic underpinnings of sex and male morph determination in a West African cichlid fish, *Pelvicachromis pulcher*, in which more acidic conditions during the first 30 days of development result in a more male-biased adult sex ratio (Heiligenberg, 1965; Reddon and Hurd, 2013). In the lab, *P. pulcher* males show four alternative morphs that are assumed to also exist in nature and are named for their opercular coloration (Linke and Staeck, 1994). The most common and best studied are "red" males and "yellow" males which represent up to 90% of the males in the lab population, and here we also include less common "green" males (but we omit "blue" males, due to their rarity). In a semi-naturalistic setting, both yellow and red males bred monogamously, but about half of red males hold harems, while no yellow males do (Martin and Taborsky, 1997). Red males are more aggressive than yellow males, while females are less aggressive still (Seaver and Hurd, 2017). Male morph was previously thought to be genetically determined and fixed for life (Heiligenberg, 1965; Martin and Taborsky, 1997), but exposure to masculinizing low pH during the critical period produces more males of the more aggressive, haremic-tending, red morph; up to 70% compared to 13% at neutral pH conditions (Reddon and Hurd, 2013) with no published evidence for adult plasticity. The degree to which environmental factors and the mechanisms involved in ESD also influence the dramatic discrete within-sex phenotypic variation associated with the development of alternative reproductive tactics (ARTs) (Gross, 1996; Johnson and Brockmann, 2012; Moore et al., 1998; Taborsky et al., 2008) is largely unknown. *P. pulcher* promises to be a valuable model in which to explore the link between mechanisms of sex determination and intrasexual variation of ARTs.

In this study, we sequenced both copies of the *P. pulcher* cyp19a1 gene, and performed gene expression analysis and DNA methylation analysis in both gonad and brain tissue to compare females, two male morphs, and fry. We examined patterns of methylation in two different regions upstream of each gene and asked whether a signal of incipient sexual differentiation was present in fry tissues.

2. Materials and methods

2.1. Ethical approval

This work and all protocols were approved by the University of

Table 1
Primers used for quantitative PCR.

Gene	Primer sequence	Amplicon length	Primer Efficiency	R^2 dil. series
cyp19a1A	F: AACACAGGCCGAATGCACCGC R: GCGAGGGCCTGAACCGAATGG	113 bp	69.5%	0.998
cyp19a1B	F: ACTACTTTGAGACCTGGCAAACAG R: GCTCTCCATCGCATCTTGCAG	116 bp	45.0%	0.977
GAPDH	F: TTCCGTGTTCCCACCCCCAA R: TGGGTCCATTAGAGGCTTCCTTCA	112 bp	39.1%	0.985

Alberta Biological Sciences Animal Policy and Welfare Committee (protocol number 00000055) and adhere to the guidelines of the Canadian Council for Animal Care. All euthanasia necessary for tissue collection was conducted using tricaine methanesulfonate (MS-222), and no other experimental conditions causing stress, harm or anesthesia were involved. All fish were descended from store-bought fish intended for the hobby trade assumed to have been in captivity for multiple generations.

2.2. Animal husbandry and sampling

Sexually mature adults were sampled from the lab stock population for DNA and RNA. Brains and gonads were dissected and placed in 95% EtOH for DNA (females: n = 4; yellow males: n = 5; red males: n = 4; green males: n = 4) or in RNAlater (Thermo Fisher) for RNA (females: n = 4, yellow males: n = 4, and red males: n = 4; the less common green males were not available at the time of RNA sampling and therefore not included).

Fry were obtained from adult breeding pairs of yellow males and females (n = 3) from the lab stock population and housed in ten-gallon tanks with sand substrate, a bubble filter, a plastic plant and three terracotta pot shards for cover at constant temperature (24 ± 2 °C) and neutral pH (7.0 ± 0.5) with 30% water changes every 1–3 days to maintain pH. These conditions are expected to produce a sex ratio of approximately 20% male (Rubin, 1985; Reddon and Hurd, 2013). Spawning took place within a month producing species-typical brood sizes of approximately 30–50 fry. Males were removed at 11 days post-spawning, while females were kept with their fry. Fry were sacrificed at day 30, as pH exposure prior to this age influences sex and morph determination (Reddon and Hurd, 2013). Precise timing of gonad development in this species is not known, but this is the end of the critical period for ESD in Apistogramma cichlids (Römer and Beisenherz, 1996). Fry from a single brood of each breeding pair were individually euthanized and, given the difficulty of dissecting brain and gonad tissue from 30 day old fry, were divided in half (head and trunk) (Heule et al., 2014a) without histological analysis of the presumptive gonads and placed in 95% EtOH for DNA (n = 3–5 per brood) or in RNAlater (Thermo Fisher) for RNA (n = 3–5 per brood). Separate individuals were used for DNA and RNA for technical reasons to ensure that the DNA and RNA samples obtained were high quality.

2.3. Gene and promoter sequencing

The *P. pulcher* cyp19a1A and cyp19a1B genes and their upstream intergenic regions were Sanger sequenced using both degenerate and non-degenerate primers designed to regions conserved among other cichlid species, and gaps were filled by sequencing with *P. pulcher*-specific primers (GenBank: MN178255, MN178256). Open reading frames and transcription start sites were predicted with Geneious v5.6.5 (https://www.geneious.com) and exon locations were predicted with the GeneWise tool (https://www.ebi.ac.uk/Tools/psa/genewise/) based on Nile tilapia sequences (NP_001266515.1 and NP_001266519.1). All CpG sites were identified in each upstream region.

2.4. Quantitative real-time PCR (qPCR)

To measure aromatase gene expression, we performed RT-qPCR on RNA samples from fry head and trunk samples as well as male and female adult gonadal and brain tissues including yellow and red males to address the alternate male phenotypes. Total RNA was extracted (Maxwell 16: Promega), DNase treated (TURBO DNA-free: Invitrogen), quantified by Nanodrop (Thermo Scientific) and checked for integrity by ethidium bromide gel. Approximately 100 ng of RNA was reverse transcribed in a 20 µl reaction (SuperScript III; Invitrogen). qPCR was conducted for cyp19a1A, cyp19a1B and the reference gene GAPDH (genbank accession AF520612.1) (primers: Table 1) with duplicate 20 µl qPCR reactions including 4 µl cDNA template (diluted 1:4 with water), forward and reverse primers (each at 500 nM), and Roche LightCycler 480 SYBR Green master mix. The amplification protocol (CFX Connect real-time PCR instrument; Bio-Rad) included a denaturation (10 min at 95 °C) followed by 40 cycles of 10 s at 95 °C, 20 s at 70 °C, 30 s at 72 °C, and optical detection each cycle, and a melt curve from 65 °C to 95 °C in 0.5 °C steps. To account for primer efficiency, each gene in each sample was quantified against a five-step four-fold dilution series of a pooled sample template that was a mixture of fry, adult male, and adult female RNA. To obtain a relative expression level for cyp19a1A and cyp19a1B, these quantities were normalized in reference to the quantity of GAPDH in each sample, thereby accounting for the low primer efficiency in a manner analogous to a delta/delta CT calculation, and allowing relative comparison of expression level for cyp19a1A and cyp19a1B within tissue. Comparison of gene expression level between tissues should be viewed conservatively because GAPDH may be expressed at different levels in brain and gonad.

2.5. Methylation assay

2.5.1. Bisulfite amplicon sequencing

We used amplicon sequencing, previously validated for methylation analysis (Bernstein et al., 2015; Masser et al., 2015), which allows quantification of methylation patterns as well as overall percent methylation. Genomic DNA was extracted by proteinase K digestion and phenol:chloroform purification. Approximately 500 ng of each genomic DNA sample was bisulfite treated (Zymo Research EZ Methylation-Gold kit), converting cytosine to uracil but leaving methylated cytosines intact. Upon PCR amplification and subsequent sequencing, the converted bases are read as thymine. First round PCR (PCR-1) with locus-specific primers designed with MethylPrimer Express including Illumina compatible ends (Figs. 1 and 2; Table 2) amplified two regions of each aromatase gene upstream intergenic region, one proximal to the transcription start site (AP, BP), similar to studies performed in other fish species (Navarro-Martin et al., 2011), and a second toward the middle of the intergenic region (AI, BI) as this area contains numerous transcription factor binding sites (Böhne et al., 2013) but has not previously been included in methylation studies.

This information from previous studies was taken into consideration when selecting sites to target in the current study. We also attempted to target regions with a high density of CpG sites. As applied to methylation analysis, the amplicon strategy is constrained by the ability to design and optimize primers that cannot span a CpG and must anneal

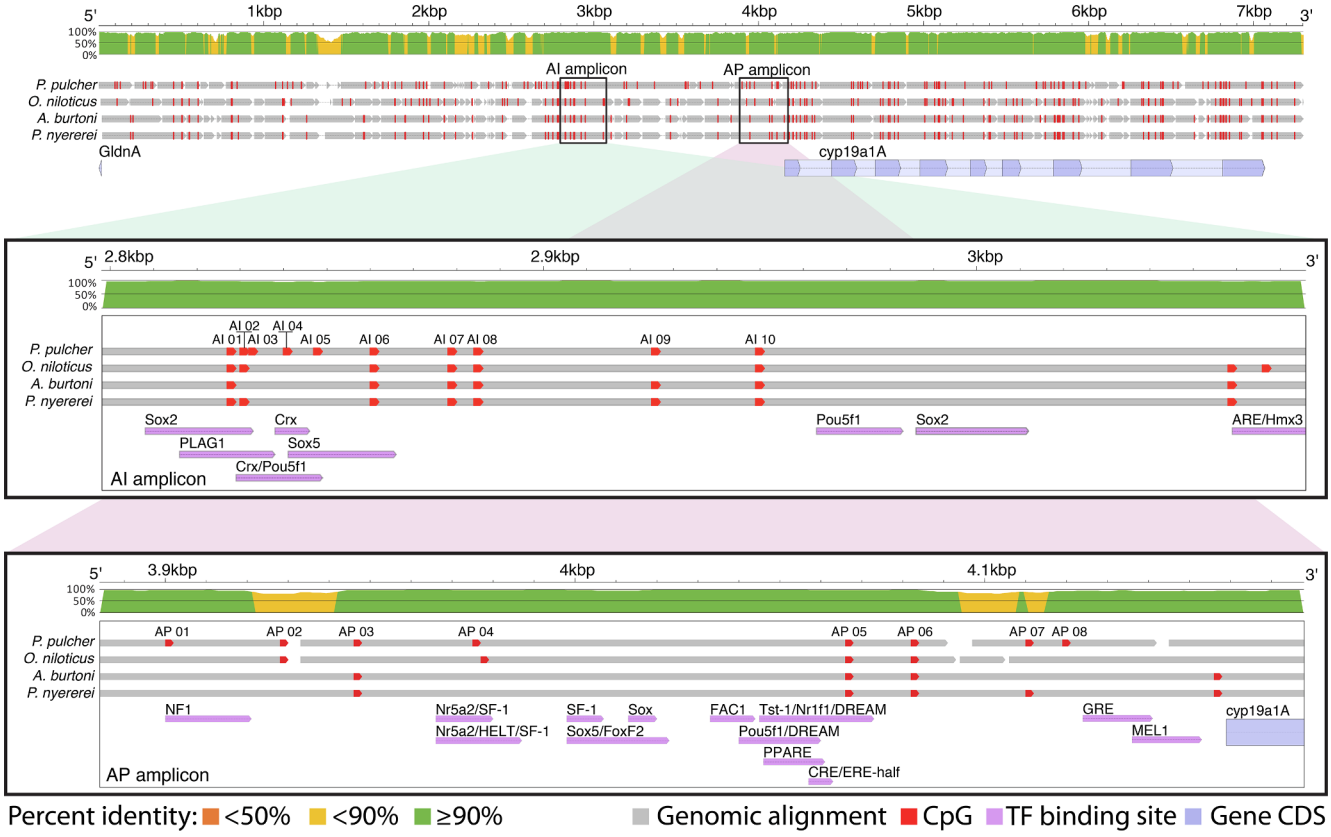

Fig. 1. Multiple sequence alignment for cyp19a1A and upstream genomic region. Genomic sequence was aligned using Geneious alignment algorithm in v5.6.5. Gene CDS alignments were derived from *O. niloticus* versions of *aromatase* (NP_001266515.1) and *gliomedin A* (XP_005463224.1). Binding sites within amplicon regions were adapted from Böhne et al (2013). Sequence percent identity was calculated using all unambiguous bases at each site and was smoothed within a 20 bp window. Base pair coordinates refer to the length of the multiple sequence alignment and includes gaps in genomic sequences.

Table 2
Primers used for amplification from Bisulfite converted gDNA.

Amplicon	Primer sequence[†]	Amplicon length	Annealing temp °C
AI	F: TGTTTTTTAGGAGAAATAAAGGG R: TGTTTTTTAGGAGAAATAAAGGG	277 bp	58.4
AP	F: TAGTTGAAAATTTTTTYGTTAATAAA R: CAAACAAAAATCAAATCCATAA	280 bp	56.1
BI	F: TTTGTGTTAAAGGAGGTAAGGA R: CTAATTTCAAAACCAAACCAAC	320 bp	62.4
BP	F: AAGAAGGTAATAGGAAGGTTATTTA R: TCTCCAAATAATAAAAAACAACA	259 bp	60.0

[†]Forward primers included the 5′ Illumina compatible end TCGTCGGCAGCGT CAGATGTGTATAAGAGACAG and reverse primers included the 5′ Illumina compatible end GTCTCGTGGGCTCGGAGATGTGTATAAGAGACAG.

specifically despite the reduced sequence complexity that results from bisulfite treated DNA that converts all non CpG Cs to T. The AI and AP amplicons span 10 and 7 CpGs respectively. One additional CpG embedded in the AP forward primer was excluded from analysis. The BI amplicon and BP amplicons span 4 and 7 CpGs respectively with 3 of the CpGs in BP amplicon downstream of the predicted transcription start site.

PCR-1 was carried out in 50 µl reactions using Immomix (Bioline), with 10 ng of bisulfite treated template DNA and primers (Table 2) at 0.8 µM each. The amplification protocol included a denaturation (95 °C for 10 min) and an initial 5 cycles of 95 °C for 30 s, 30 s at the amplicon-specific annealing temperature (Table 2), and 72 °C for 10 s, followed by 45 cycles of 95 °C for 30 s, 67 °C for 30 s, and 72 °C for 10 s, and 72 °C for 10 min. Fragments were visually checked by gel before and after magnetic bead cleanup (PCRCLEAN DX, Aline Biosciences). Sample-specific barcodes were added in a second round of PCR (PCR-2) in 25 µl reactions using Phusion HF (NEB), with 4 µl purified PCR-1 product as template and Nextera index primers (Illumina) at 0.1 µM according to manufacturer's protocol. The amplification protocol included denaturation (98 °C for 2 min) followed by 8 cycles of 98 °C for 10 s, 53 °C for 30 s, and 72 °C for 15 s, and 72 °C for 5 min.

PCR-2 products were visually checked on a gel and quantified with SYBR Green dye (Invitrogen) in 96 well format (Twinkle LB970; Berthold Technologies). Barcoded samples for all 4 amplicons from up to 95 samples (including experimental samples described elsewhere) were pooled at equal concentrations, column purified (Qiagen) and quantified (NanoDrop 1000, Marshall Scientific). Each pooled sample was diluted to 10 nM, spiked with 10% PhiX to increase library complexity, and sequenced on one of two runs on the MiSeq platform (Illumina) using V2 sequencing chemistry to produce 250 bp paired-end reads.

2.5.2. Computational analysis of methylation data

Using Bowtie2 v2.2.9 (Langmead and Salzberg, 2012), paired forward and reverse reads were aligned to reference amplicon sequences that were *in silico* bisulfite converted (Cs converted to Ts) with Bismark genome preparation software v0.15.2 (Krueger and Andrews, 2011). At CpGs, samtools v1.9 mpileup (Li et al., 2009) and custom Python scripts were used to count the number of Cs (methylated) versus Ts (unmethylated) at each CpG to calculate percent methylation (C/(C + T)*100). At non-CpG C bases, the frequency of Ts revealed 99.25% ± 0.16% bisulfite conversion completeness, on par with previous reports (96%: Wang et al., 2017; 98%: Navarro-Martin et al., 2011). For non-C bases, the frequency of incorrect nucleotides revealed

a sequencing error rate of 0.62% ± 0.33%.

To determine whether the methylation states of multiple CpGs were linked, we analyzed the specific methylation pattern along each read of each amplicon, termed the "epiallele". Paired forward and reverse reads were merged using FLASH2 v1.2.11 and aligned to the *in silico* bisulfite converted amplicon sequences with Bowtie2. Multiple alignment of reads was carried out with MUSCLE v3.8.31 (Edgar, 2004) and for each amplicon and each sample, custom python scripts and usearch v5.2.236 (Edgar, 2010) were used to count the number of occurrences of each unique epiallele. We report only on the methylation state of each CpG in the amplicon and do not analyze the full region for genetic polymorphisms.

2.6. Statistical analyses

Statistical tests and visualization were carried out in R version 3.6.0 (R-Core-Team, 2017). Data manipulation was performed using base R and packages stats, dplyr (Wickham et al., 2018), and reshape (Wickham, 2007). Linear models, ANOVAs, and principal component analyses were all performed using the package stats. Mixed-effect models were conducted using the lme4 and lmerTest packages (Bates et al., 2015; Kuznetsova et al., 2019) and the emmeans package (Lenth et al., 2019) for post-hoc Tukey HSD tests. Fixed effects models were conducted with the Anova function from the car package (Fox and Weisberg, 2019) and TukeyHSD from the stats package.

3. Results

3.1. Gene structure

The final genomic regions assembled encompass a 7001 bp and a 6126 bp sequence containing the gene and upstream intergenic region for cyp19a1A and cyp19a1B respectively (Figs. 1 and 2). The predicted aromatase coding regions span 2860 bp (cyp19a1A) and 2717 bp (cyp19a1B), including introns, while the upstream intergenic sequences are 3434 bp (cyp19a1A) and 2142 bp (cyp19a1B) in length. For each gene, the upstream neighbor, transcribed from the opposite strand, is a copy of the gliomedin gene, a ligand for neurofascin known to function at the nodes of Ranvier in mammals (Eshed et al., 2005). The aromatase genes themselves are structurally conserved. Both have 9 exons and relatively short introns, similar to other fishes (Tanaka et al., 1995).

To initiate a study of epigenetic regulation, we focused on CpG sites, which present the opportunity for DNA methylation. The intergenic upstream region of the A-copy is relatively CpG dense with a total of 117 sites while the intergenic upstream region of the B-copy is relatively CpG sparse with only 23 sites. For the A-copy and the B-copy respectively, 48 and 3 of the CpGs are conserved across the cichlid species for which sequences of this region were available at the time (Nile tilapia*, Astatotilapia burtoni, Pundamilia nyererei*), while 63 of the 117 CpG sites in the A-copy intergenic region and 9 out of the 23 CpG sites in the B-copy region are shared with at least one of the three available cichlid sequences. Using an amplicon sequencing strategy that targets short regions in the genome, we assessed methylation state for 17 of the 117 CpGs from the A-copy upstream intergenic region and 8 of the 23 CpGs from the B-copy upstream intergenic region. Three of the surveyed CpGs in the A-copy region were polymorphic. At a conservative estimate, 5 adult males, including all color morphs, were heterozygous (C/G) for the fifth CpG in the AP amplicon (AP05); 5 fry from one brood were heterozygous (C/T) for the second CpG in the AI amplicon (AI02); and 4 fry from another brood were heterozygous (C/T) for the tenth CpG in the AI amplicon (AI10), out of 30 individuals total. The two polymorphisms in the intergenic amplicon were recognized in individuals in specific broods with roughly 50% more T's than other samples, which would be incorrectly interpreted as bisulfite converted unmethylated bases. While potentially very interesting, these polymorphic CpGs were not detected in any of our adult samples and were therefore omitted from any further analysis.

Although we did not perform functional analyses, we note that based on alignment to other cichlid species (Böhne et al., 2013) our amplicons span several conserved putative binding sites for transcription factors implicated in sex determination and differentiation (Figs. 1 and 2). The AP amplicon includes, among others, binding sites for sf-1 and Sox5, while AI includes a binding site for Sox5 and two Sox2 binding sites, one of which spans a conserved CpG. The BI amplicon similarly includes a Sox2 binding site, though it was removed from the CpG analysis for being 3′ to the gene start site.

3.2. cyp19a1A and cyp19a1B gene expression

3.2.1. Adult expression

We analyzed log transformed expression of the A-copy and B-copy transcripts relative to GAPDH with qRT-PCR using type-II ANOVAs with tissue type (brain, gonad) and sex/color morph (female, red male, yellow male) as fixed effect factors (Table 3, Fig. 3). Post-hoc Tukey HSD tests provide the specific comparison p-values reported.

We found the expected increase in expression of the A-copy in ovaries relative to testes (post-hoc group comparisons, ovaries relative to yellow males: $p = 0.0008$; relative to red males: $p < 0.0001$, Fig. 3A) but no difference between yellow and red males (post-hoc group comparison $p = 0.90$). We found no difference between adults in the expression of the A-copy in brain tissue (all post-hoc group comparisons $p > 0.99$, Fig. 3B). In red, but not yellow males, expression of the A-copy was lower in testes than in brain tissue (red: $p = 0.009$; yellow: $p = 0.29$).

In adults, the B-copy also followed the conventional teleost pattern, being expressed more strongly in the brain than gonads ($p < 0.0001$, Fig. 3C & D). While the effect was strongest in females, it was also seen in both yellow and red male morphs (all $p < 0.0001$). There were no significant differences between the sexes/morphs in expression of the B-copy in brain tissue (all $p > 0.43$, Fig. 3D), nor were there any sex or morph differences in B-copy expression in gonads (all $p > 0.90$, Fig. 3C).

3.2.2. Fry expression

We analyzed expression of both A and B copies in fry following the same methods applied to adults, except that mixed effects models were used to incorporate random effects terms for fry brood and assay plate, while the fixed effects were limited to tissue type (head, trunk) since the fry had no identified sex (fixed effects reported in Table 3). Post-hoc Tukey HSD tests provide the specific comparison p-values reported.

We found a non-significant increase in expression of the A-copy in the trunk (gonads) of day 30 fry relative to heads ($p = 0.44$). A-copy expression was dramatically lower than B-copy expression in both trunk and head (both $p < 0.0001$) suggesting that the gene may not yet be active. We did find significantly higher in expression of the B-copy in the heads (brain) relative to trunk ($p < 0.0001$, Fig. 4, Table 3). For both genes, the expression level calculated relative to GAPDH is an order of magnitude lower in the fry samples than in adult samples, likely due to the dilution of aromatase mRNA in these mixed tissue samples.

3.3. Percent methylation

We measured methylation at CpG sites in brain and gonad tissues from adults and fry for the four different amplicons (AI, AP, BI and BP) using different adult individuals for the methylation analyses from those assayed for gene expression for technical reasons, and testing head and trunk tissue from 30 day old fry from different individuals but the same broods assayed for gene expression. We expected to find reduced methylation in tissues and sexes for which we saw increased aromatase expression.

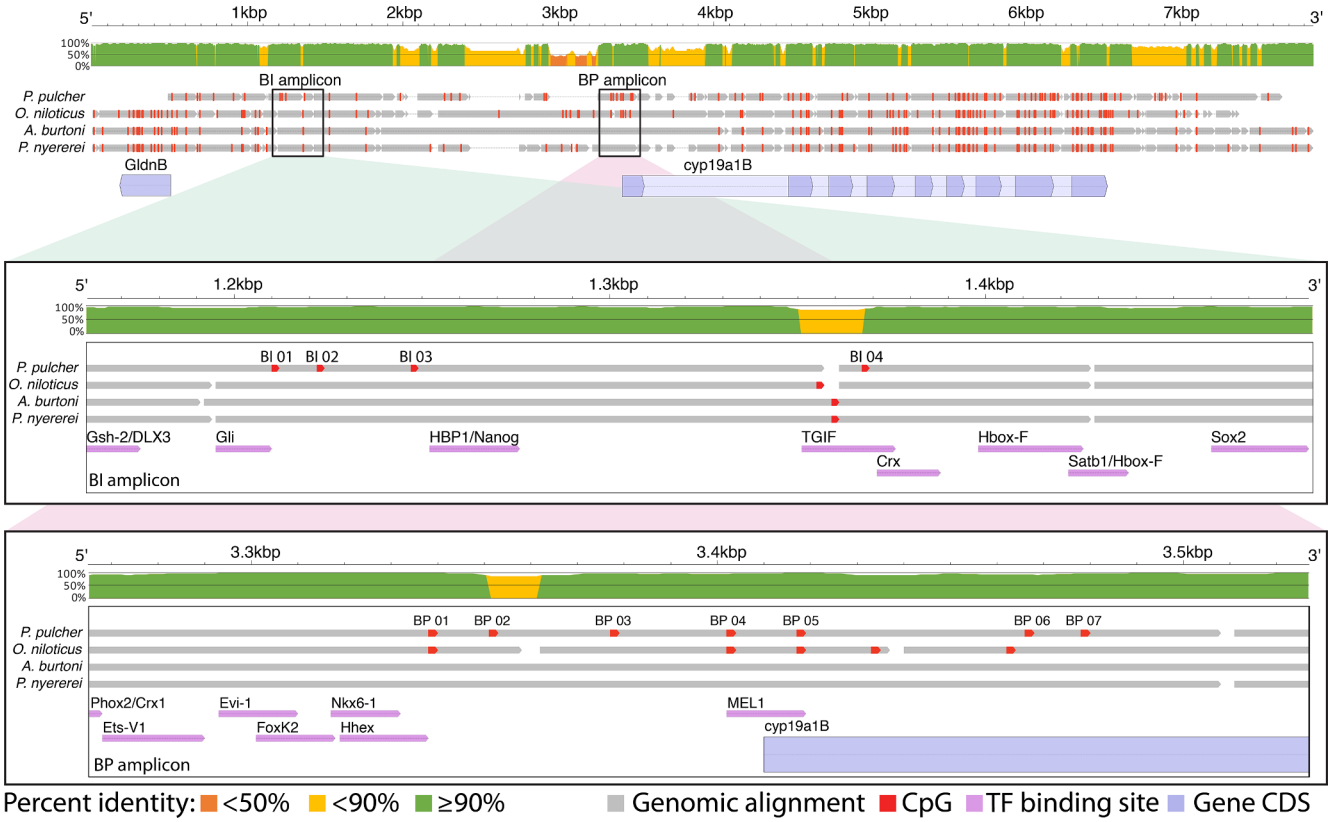

Fig. 2. Multiple sequence alignment for cyp19a1B and upstream genomic region. Genomic sequence was aligned using Geneious alignment algorithm in v5.6.5. Gene CDS alignments were derived from *O. niloticus* versions of *brain aromatase* (NP_001266519.1) and *gliomedin B* (uncharacterized protein LOC100693335: XP_003443992.2). Binding sites within amplicon regions were adapted from Böhne et al. (2013). Sequence percent identity was calculated using all unambiguous bases at each site and was smoothed within a 20 bp window. Base pair coordinates refer to the length of the multiple sequence alignment and includes gaps in genomic sequences.

Table 3
Gene Expression ANOVA Tables.

Adult		Sum Sq	F (df)	p-value
A-copy	Tissue	0.0039	0.0097 (1,13)	0.92
	Sex/Morph	17.1	21.27 (2, 13)	< 0.0001
	Tissue × Sex/Morph	19.8	24.6 (2,13)	< 0.0001
	Residuals	5.2		
B-copy	Tissue	87	265 (1,15)	< 0.0001
	Sex/Morph	1.4	2.2 (2,15)	0.15
	Tissue × Sex/Morph	0.1	0.2 (2,15)	0.81
	Residuals	4.9		
30 day Fry			t (df)	p-value
A-copy	Tissue		3.39 (1,21.0)	0.003
B-copy	Tissue		18.4 (1,21.1)	< 0.0001

3.3.1. Percent methylation in adults

Percent methylation was analyzed for each amplicon as a function of tissue type (brain, gonad), and sex/morph (female, yellow male, red male, green male) using type-II ANOVAs (Table 4). Post-hoc Tukey HSD tests provide the specific comparison p-values reported.

Percent methylation in both the AI and AP amplicons showed significant effects of sex/morph, and an interaction of sex/morph with tissue; gonadal tissue was significantly more methylated than brain tissue in the AI but not AP amplicon (Table 4, Fig. 5). Given the strong ovarian expression of the A-copy, we expect decreased methylation of this enhancer in female gonad samples. Females did indeed show the expected reduction in methylation relative to males of each color/reproductive morph for the AI (all three post-hoc group comparisons, $p < 0.0001$ Fig. 5A) and to a lesser degree the AP amplicons ($p < 0.0005$ Fig. 5B) in the gonads. Methylation levels were lower in ovarian tissue than in female brain tissue (AI $p = 0.09$, AP $p = 0.004$), but higher in testicular tissue than brain (all male AI comparisons $p < 0.0001$; AP comparisons $p = 0.33, 0.03, 0.51$ for yellow, red, and green respectively). We found no significant differences between any of the male morphs for percent methylation in either tissue (all $p > 0.30$).

We did not have strong expectations for sex-specific methylation status of the A-copy promoter in brain tissue, since it is not expressed in this tissue for either sex. Surprisingly, for a gene that is turned off, there was low methylation (50% or less) of the AI amplicon (Fig. 5C). The uniformly high methylation level of the AP amplicon (Fig. 5D) is more consistent with the expectations for a gene that is turned off (Dunham et al., 2012; Jones, 2012). These results indicate a tissue-specific enhancer influenced by methylation in the AP region that is sufficient for reducing A-copy expression in the brain, as well as a sex-specific enhancer influenced by methylation in the AI region that is responsible for reducing A-copy expression in the male testes.

Percent methylation in B-copy CpG sites was higher in gonadal than brain tissue in the BI amplicon, but otherwise showed no significant differences between tissues or sexes/morphs (Table 4, Fig. 6,). Given the elevated expression of the B-copy in brains, we predicted low levels of methylation for amplicons BI and BP in brain tissue. This is evident for the BI amplicon where methylation averages approximately 50% (Fig. 6C), but less so for BP (Fig. 6D). Given the uniformly minimal expression of the B-copy in the gonads, we predicted high levels of methylation across all samples, which was somewhat the case, though we again observed variation (Fig. 6). Inexplicably, while methylation

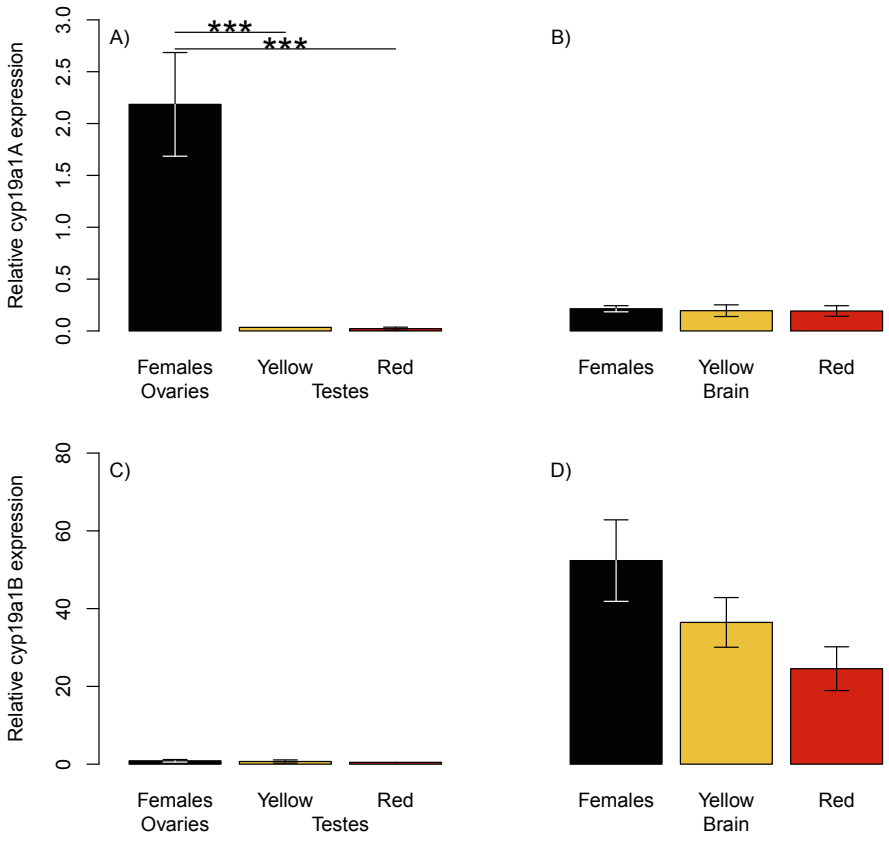

Fig. 3. Relative aromatase gene expression for the A-copy (A & B) and B-copy (C & D) assayed in adult gonad (A & C) and brain (B & D) tissue by qPCR, normalized against GAPDH reference gene thus y-axes within tissue are comparable (*** = $P < 0.001$).

levels of the B-copy amplicons do not appear to explain expression, the level of methylation between intergenic, BI (Fig. 6A), and proximal, BP (Fig. 6B), amplicons and the decreased methylation in female ovaries, though not statistically significant, parallels the pattern seen for the A-copy amplicons.

3.3.2. Percent methylation in 30-day fry

We analyzed differences in mean CpG methylation between tissues (head vs. trunk) for each of the four amplicons using an analysis of variance that included the fry's brood as a random effect (Table 5, Fig. 7). Given the low A-copy expression in both fry tissues, we considered the possibility of elevated methylation rather than the canonical demethylation associated with expression in ovaries. We did expect to see reduced methylation in B-copy amplicons for head tissue where expression was elevated.

We found relatively high methylation in the AP amplicon, and no significant difference between the two tissues (Fig. 7B). However, counter to our predictions, we found a very strong effect in the opposite of the predicted direction for the AI amplicon (Fig. 7A), with low methylation levels in head tissue relative to trunk. Methylation was higher in the fry AP amplicon than AI (mixed-effect ANOVA with tissue and amplicon as fixed effects, and individual as a random effect, main effect of amplicon $F_{(1,46)} = 230.0$, $p < 0.0001$).

For both of the B-copy amplicons, we saw the anticipated reduction in methylation in head tissue where the gene is expressed, but not to the point of statistical significance (BI $p = 0.28$, BP $p = 0.11$, Table 5, Fig. 7). Similar to the A-copy amplicons in fry, the amplicon proximal to the gene showed overall higher levels of methylation (Fig. 7C) than the intergenic amplicon (Fig. 7D) (mixed-effect ANOVA with tissue and amplicon as fixed effects, and individual as a random effect, main effect of amplicon $F_{(1,46)} = 18.0$, $p < 0.0001$).

3.4. Variation in methylation patterns

Across tissues and sexes, the mean level of methylation among adults in the A-copy promoter conformed to predictions based on gene expression. Because the regulation of gene expression occurs on a per-chromosome basis, with each chromosome having just one set of methyl marks, the specific pattern of methylated and unmethylated CpGs (the epiallele) may be important. We investigated whether epialleles were of particular importance in the gonads. With six CpG sites in the AP amplicon and eight in the AI amplicon there are 64 and 256 possible epialleles included in our analysis, 63 and 250 of which were seen in our adult gonad samples. We compared the frequencies at which epialleles were found in samples from ovaries and testes adult females and males. Sex differences in epiallele frequency ($p < 0.05$ in a *t*-test) were found in 53 of 313 (16.9%) of A-copy epialleles (not all possible epialleles were present), which is far above the expected 5% rate under the null hypothesis (binomial test $p \ll 0.0001$). This contrasted with the 0.02% of B-copy epialleles showing sex differences in gonads, and the on 5.01% and 4.2% of epialleles showing sex differences in the brain (A-copy and B-copy respectively), binomial tests all $p > 0.17$. Since we find no evidence of sex differences in epialleles outside of the A-copy in gonads we restrict further analysis to this gene and these tissues.

We found three epialleles of the AP amplicon and nine epialleles of the AI amplicon which differ in frequency of occurrence between ovaries and testes after FDR correction and which comprise at least 1% of the reads for a sample on average (Table 6). Two of the sex-biased AP epialleles are testes-biased and one ovary-biased. Of the nine sex-biased AI epialleles, six are more common in testes, and three more common in ovaries. As expected for a gene that is expressed primarily in ovaries, the female-biased epialleles included the all-unmethylated epialleles and those in which all but one CpG is unmethlyated (read as Ts), while the male-biased epialleles included those that are fully methylated, and

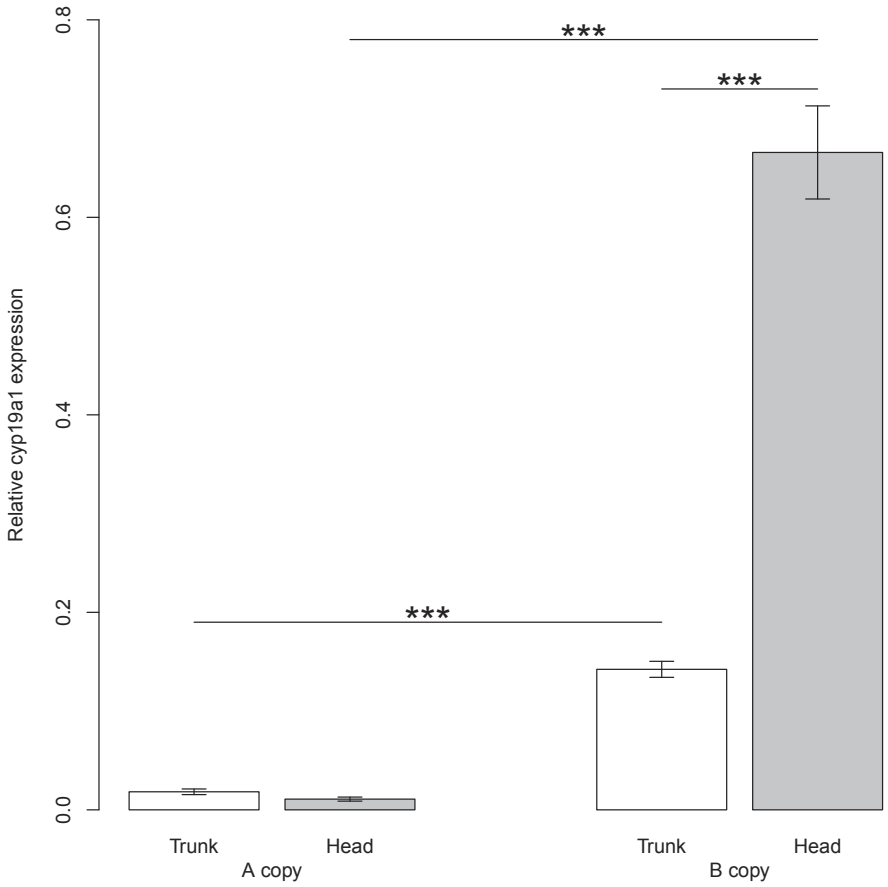

Fig. 4. Relative aromatase gene expression for the A-copy (left) and B-copy (right) assayed in fry trunk (white) and head (grey) tissue by qPCR, normalized against GAPDH reference gene (*** = P < 0.001).

Table 4
Percent Methylation ANOVA Tables; Adult tissues.

Amplicon		Sum Sq	F (df)	p-value
AI	Tissue	6643.9	212.6 (1,24)	< 0.0001
	Sex/Morph	4077.7	43.5 (3,24)	< 0.0001
	Tissue × Sex/Morph	4596	49.0 (3,24)	< 0.0001
	Residuals	749.9		
AP	Tissue	57.8	2.8 (1,24)	0.105
	Sex/Morph	427.8	7.0 (3,24)	0.0015
	Tissue × Sex/Morph	767.5	12.6 (3,24)	< 0.0001
	Residuals	488.3		
BI	Tissue	7257	17.1 (1,24)	0.00037
	Sex/Morph	2347.5	1.84 (3,24)	0.17
	Tissue × Sex/Morph	1792.1	1.41 (3,24)	0.27
	Residuals	10,195		
BP	Tissue	313.6	2.18 (1,24)	0.15
	Sex/Morph	878.1	2.04 (3,24)	0.14
	Tissue × Sex/Morph	1163.9	2.7 (3,24)	0.068
	Residuals	3447.6		

those in which all but one CpG is methylated (read as C). The only exception was the female-biased AP epiallele in which the three 5′ CpGs were methylated and the three 3′ CpGs were unmethylated. The most common epialleles in our data included the male-biased all-methylated epialleles of AP (average 65.6% of the reads per male sample) and AI (average 47.6%) as well as the female-biased all-unmethylated epiallele for AI (average 53.8% of reads per female sample). The all-unmethylated epiallele for AP, while female-biased, did not differ significantly in prevalence between males and females, which is consistent with the interpretation of AP as a tissue-specific rather than sex-specific promoter region.

The most common epialleles in our fry samples were the all-methylated epialleles for both the AP (average 62.5% of reads per sample) and AI amplicons (average 38.2%). Although the A-copy is not expressed at a high level in the trunk of these fry at day 30, and the overall methylation for fry trunk samples was 90% for AP and 75% for AI amplicons (Fig. 7), we were interested to know whether the variation for the proportion of different epialleles among individual fry reflected the sex biases seen in adult gonads. To assess individual variation among fry, we performed PCA and identified seven epialleles that were weighted heavily (> 2 standard deviations from the mean) on the first two principal components (Table 6, Fig. 8), which combined which account for 54.8, and 13.4% of the variation (respectively) among fry. These seven epialleles were all found in > 2% of the total reads among fry, and four of them (all-methylated for AI and AP, all-unmethylated for AI, and the AP epiallele in which the three 5′ CpGs are methylated and the three 3′ CpGs are unmethylated) were among those that were highly represented and significantly sex-biased in adults. While highly explanatory of PC2, the all-unmethylated epiallele indicative of female ovaries (average 53.8% of reads per female sample) is found in only an average of 5.8% of the epialleles in fry samples. Across all A-copy epialleles, there was a significant negative correlation between the size effect of the difference between ovary and testicular expression in adults and PC1 scores in trunk tissue in fry (Spearman's rho = −0.118, p = 0.037), the effect was even stronger on fry trunk PC2 scores (Spearman's rho = −0.244, p < 0.0001).

Taken together, these results show that the epialleles which differ most strongly between ovaries and testes in adults are also those which show the greatest variation in the trunk tissue of 30 day-old fry. This suggests that despite the tissue complexity, immature state of the

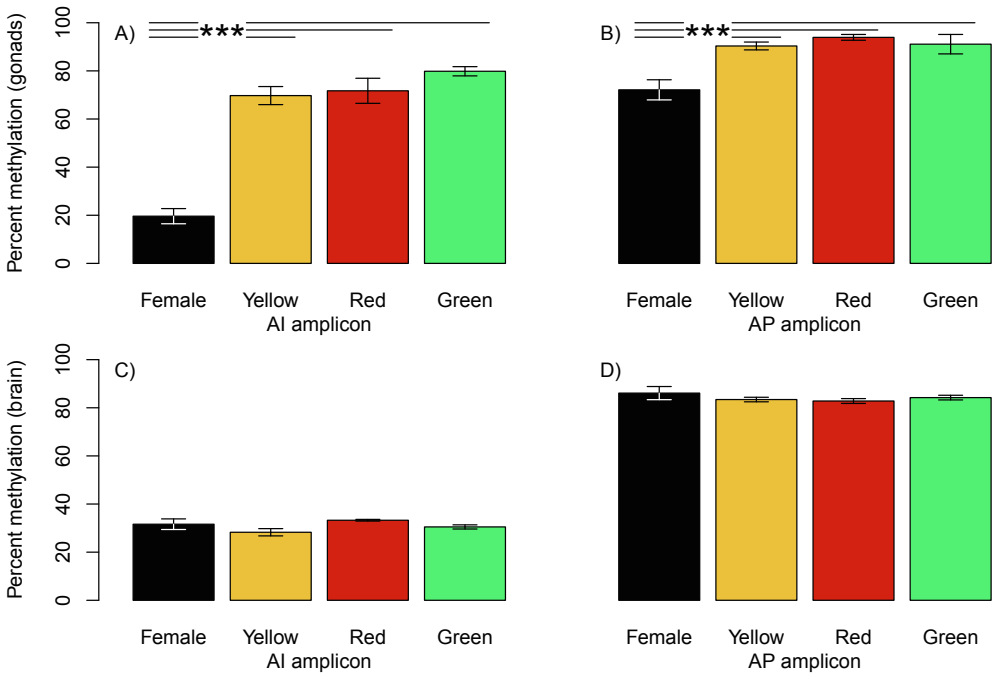

Fig. 5. cyp19a1A gene promoter percent methylation for the two A-copy amplicons, AI (A & C) and AP (B & D), for adult gonad (A & B) and brain (C & D) samples from females (black) and male morphs (colored accordingly). Asterisks indicate significantly different expression between females and male morphs (*** = P < 0.001).

gonads at day 30, and lack of A-copy expression, we are still able to detect the epigenetic marks of sex determination on the A-copy promoter.

4. Discussion

Here, we sequenced the promoter and coding region for both the brain and the gonad copies of the aromatase gene from a cichlid fish species, *Pelvacachromis pulcher,* in which pH (and possibly other environmental factors) is known to influence sex ratio as well as male morph proportions, and we examined tissue and sex differences in their expression and their promoter methylation state. Similar studies, conducted for species with TSD, reveal environmental effects at the epigenetic and transcriptomic level that vary between and within sex. Functional studies, such as that in the red-eared slider turtle (Ramsey et al., 2007), demonstrate that temperature-based female-biased cyp19a1 expression is attributable to demethylation impacting binding sites for FOX and SF-1 transcription factors and the TATA box in the

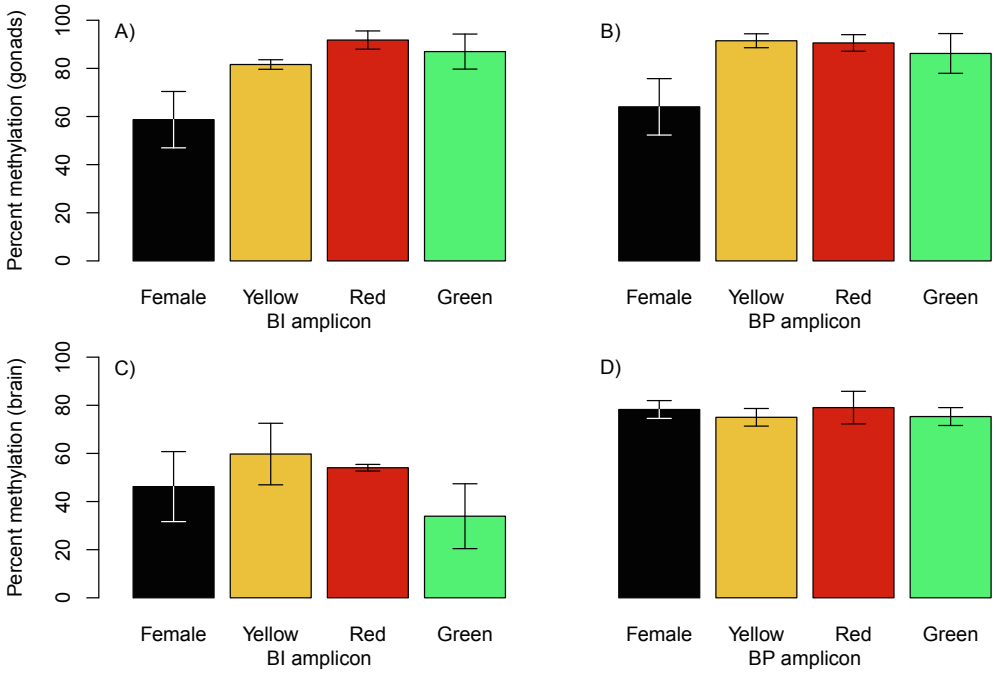

Fig. 6. cyp19a1B gene promoter percent methylation for the two B-copy amplicons, BI (A & C) and BP (B & D), for adult gonad (A & B) and brain (C & D) samples from females (black) and male morphs (colored accordingly).

Table 5
Percent Methylation ANOVA Tables; Fry tissues.

Amplicon			t (df)	p-value
AI	Tissue	680.4	149.8 (1,22)	< 0.0001
	Residuals	99.9		
AP	Tissue	36.4	2.46 (1,22)	0.13
	Residuals	324.8		
BI	Tissue	338	1.23 (1,22)	0.28
	Residuals	6073		
BP	Tissue	207.6	2.71	0.11
	Residuals	1685.5		

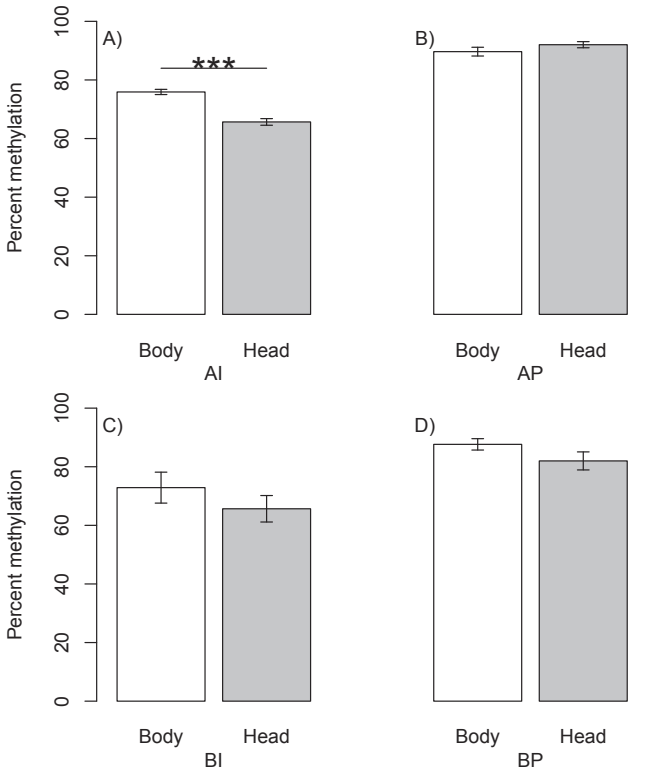

Fig. 7. Aromatase gene promoter percent methylation for both of the A-copy (A & B) and the B-copy (C & D) amplicons assayed for 30-day old fry trunk (white) and head (grey) sample (*** = P < 0.001).

promoter region upstream of cyp19a1 (Matsumoto et al., 2013). Similarly, *in vitro* studies show temperature sensitive methylation at the A-copy impacts a flounder Nr5a2 binding site (Fan et al., 2017), the sea bass SF-1 and Foxl2 sites (Navarro-Martin et al., 2011), and cAMP binding in rice eel *Monopterus albus* (Zhang et al., 2013). The degree to which species-specific results reflect underlying differences in biology or differences in experimental approach requires further comparative and functional analyses. Data from turtles, alligators, and fish show environmental effects on the expression of several transcription factors, many of which are known to impact expression of aromatase, or themselves be regulated by estrogens justifying future genome wide analyses.

Though we did not intentionally conduct a population survey for genetic polymorphisms, we encountered several SNPs in the upstream regulatory region. Notably, three CpG sites at the A-copy locus are polymorphic. Neither of the polymorphisms in AP were present among the adult samples sequenced and the single SNP in AI occurred in all male morphs, so we have no information suggesting a functional influence. Similar to our results, SNPs are known to exist in the sea bass A-copy regulatory region, with no identified consequence for aromatase expression (Galay-Burgos et al., 2006).

4.1. Gonadal aromatase

We found expression of the A-copy to be much higher in ovaries than testes. Low levels of estrogen production via aromatization in testes is necessary for spermatogenesis (Schulz et al., 2010), but fish typically show higher expression in ovaries than testes; exceptions exist such as the Tanganyikan cichlid *Ophthalmotilapia ventralis* in which the A-copy is expressed similarly in ovaries and testes (Böhne et al., 2013). We detected no significant differences in A-copy expression among the male color morphs tested. Bluehead wrasse *Thalassoma bifasciatum* also show no difference in gonadal aromatase expression between initial phase (sneaker) and terminal phase (territorial) males (Todd et al., 2018).

We found that A-copy expression in the testes was even lower than in the brain in red males. However, others have found the opposite - A-copy expression higher in testes than brain - in five cichlid species, and no significant difference in another four (Böhne et al., 2013). Few studies have addressed the role of gonadal aromatase in teleost brain tissue, and it may simply be that the expression is level is so low relative to the extremely high level of B-copy expression (Blazquez and Piferrer, 2004; Diotel et al., 2010) that it has no functional consequence.

As expected, the overall percent methylation in gonad samples had an inverse relationship with the sex bias in expression even though different individuals were used for the two analyses; ovaries showed less methylation than testes (Fig. 9A). Epigenetic analyses of ESD have largely focused on CpG sites within 500 base pairs of the gonadal aromatase promoter (red-eared slider turtle: Matsumoto et al., 2013; European sea bass: Navarro-Martin et al., 2011; black porgy *Acanthopagrus schlegeli*: Wu et al., 2012; Nile tilapia: Wang et al., 2017; flounder: Fan et al., 2017). Our results suggest that sites farther upstream may also be involved sex-biased regulation. The sex bias in methylation percentage was even more dramatic for the AI amplicon, 1341–1065 bp upstream of the gene, than it was for the AP amplicon, 260 bp upstream to 19 bp within the gene. Methylation in female ovaries was even lower in AI than in AP.

Interestingly, we show that methylation levels in AI and AP amplicons were very different from each other in brain tissue. The very low levels of expression in brain for both sexes would lead to the expectation that A-copy methylation regulating expression in this tissue should be high, but this was true for only the AP amplicon (Fig. 9A). Methylation was uniformly low for the AI amplicon in brain. These results suggest that methylation of the region proximal to the gene is sufficient to downregulate expression of the A-copy in brain tissue. While functional studies are necessary to confirm the role of the AI amplicon region in regulating sex-biased expression of gonadal aromatase, the strong correlation is highly suggestive. Importantly, these results indicate different mechanisms or promoter sites for tissue-specific expression and sex-specific expression.

4.2. Brain aromatase

As expected, we found high levels of B-copy expression in brain tissue relative to gonads, but no significant differences between sexes or male morphs and no strong relationship with methylation level at the sites we assayed (Fig. 9B). Male-biased B-copy activity has been noted in tilapia (D'Cotta et al., 2001), but a more recent survey of cichlids showed no significant sex bias for B-copy expression in the brain (Böhne et al., 2013). Brain aromatase is often studied in conjunction with behavioral differences associated with sex change, again with inconsistent or contradictory results, highlighting the importance of species-specific functions (Black et al., 2005; Breton et al., 2015; Todd et al., 2018; Zhang et al., 2008) as well as suggesting a role for post-transcriptional regulation (Aguiar et al., 2005).

Table 6
Sex-biased epialleles in adult gonad samples.

Amplicon	Epiallele*sequence	t	df	p-value†	Female mean‡	Male mean‡	Fry mean‡	PCA§	Rotation weight#	Fig. 8 label
Sexually dimorphic epialleles										
AP	CCCCCC	−5.916	12.97	0.002	31.2	65.6	62.5	PC1	0.926	A
	CCCTTT	6.261	12.83	0.001	8.9	2.6	3.1	PC1	−0.2144	B
	CTCCCC	−4.363	11.33	0.015	1.4	5.8	2.1			C
AI	CCCCCCCC	−13.50	12.13	< 0.00001	2.5	47.6	38.2	PC2	0.244	D
	TTTTTTTT	10.06	3.62	0.013	53.8	8.6	5.8	PC2	−0.3914	E
	TCTTTTTT	5.58	11.72	0.003	4.4	2.2	1.1			F
	CCCCCCTC	−5.32	12.06	0.004	0.6	1.8	4.2			G
	TCCCCCCC	−11.93	11.47	0.00001	0.1	1.9	1.9			H
	CTTTTTTT	15.07	3.47	0.005	1.8	0.2	0.3			I
	CCCTCCCC	−4.67	10.57	0.012	0.2	1.2	2.7			J
	CTCCCCCC	−5.537	12.26	0.003	0.2	1.0	1.1			K
	CCCCTCCC	−8.534	11.57	0.0002	0.6	1.0	1.2			L
Non-sexually dimorphic epialleles with large PC1 or PC2 loadings										
AP	CCCCTT	0.41	7.32	0.69	2.1	1.8	3.0	PC1	−0.234	M
	CCCCCT	−0.51	8.38	0.62	2.9	3.5	3.8	PC2	−0.4244	N
	CCTTTT	2.62	3.19	0.07	1.5	0.2	2.2	PC2	−0.51534	P

* – Epiallele sequence C represents methylated CpG, and T represents an un-methylated CpG that is converted to T by bisufite treatment.
† – P-value corrected for false discovery rate.
‡ – Mean percentage of reads per sample for specific epiallele.
§ – Principle component on which epiallele weights for description of variation among fry trunk samples.
# – Rotation weights for those epialleles > 2 standard deviations from the mean weight.

Brain aromatase expression has also shown a mixed or contradictory relationship within sex with territorial vs. sneaker ARTs in fish, with higher B-copy expression in the brains of territorial male peacock *Salaria pavo* (Goncalves et al., 2008), black-faced blennies *Tripterygion delaisi* (Schunter et al., 2014), and bluegill sunfish *Lepomis macrochirus* (Partridge et al., 2016); the opposite effect is seen in plainfin midshipman *Porichthys notatus* (Fergus and Bass, 2013), while no significant difference is seen in wrasse morphs (Todd et al., 2018). Simply put, there is no consistent relationship between brain aromatase level and reproductive strategy. In fact, brain aromatase expression has been known to vary with the season in several vertebrate species (reviewed in: Forlano et al., 2006) and is regulated according to reproductive status in male *A. burtoni* brains (Renn et al., 2008), suggesting that expression and methylation patterns at this gene may reflect current behavioral status rather than early life experience as occurs under ESD. Compared to red males, yellow *P. pulcher* males are more female-like in behavior (Seaver and Hurd, 2017) and their B-copy expression may also tend to be more female-like, but their methylation state is not, at least for the CpGs included in our analysis (Fig. 9B).

4.3. Development

We found the B-copy expressed in the head and to a lesser extent in the trunk of fry old enough to have been impacted by the sex determining effects of the environment. However, we did not see the A-copy expression we expected to see in developing ovaries. Interestingly, while overall methylation levels of the A-copy promoter are relatively high at this developmental stage, the epialleles that distinguish testes from ovaries are among the most explanatory patterns for variation among individual fry. This suggests the potential epigenetic marking of sex prior to differentiation and expression of the A-copy in the gonads.

That we do see variation in the overall percent methylation among fry, and specifically variation among fry with regard to the prevalence of the completely unmethylated epiallele for the AI amplicon, suggests that the epigenetic mark for later expression regulation (Turecki and Meaney, 2016) may be present. While the proportion of unmethylated epialleles in fry trunk samples was much lower than detected in adult gonads, and the diversity of epialleles present was higher, this is likely due to the tissue complexity introduced with crude bisection of the fry into head and trunk without dissection of brain and gonads.

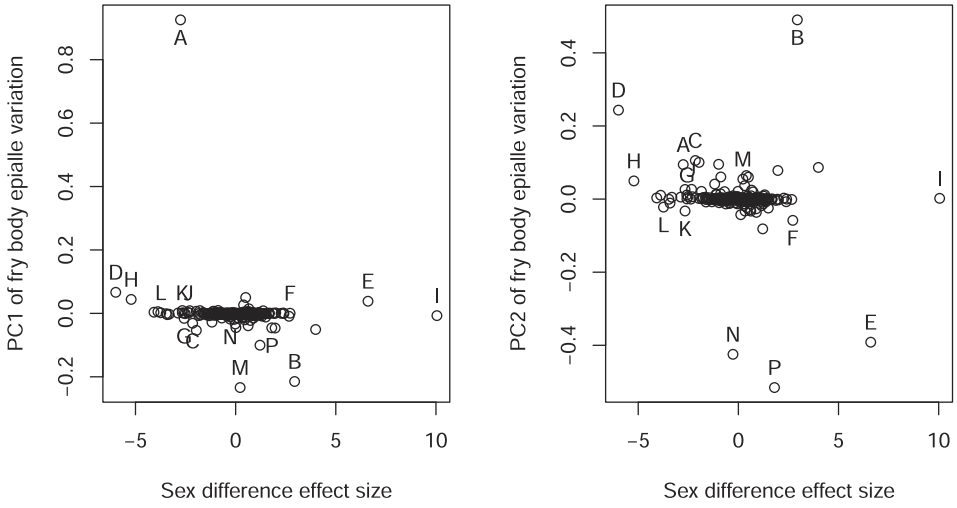

Fig. 8. PC1 (A) and PC2 (B) factor loadings for epiallele variation fry trunk as a function of the effect size for the adult sex-bias of each epiallele in gonad. Effect size is calculated as the difference in means (ovaries minus testes) divided by the pooled standard deviation so negative effect sizes indicate a testis-bias and positive values indicate ovary-bias. Labelled points refer to Table 6 and indicate epialleles found in at least 1% in the reads, that also show significant sex-bias (points A-L) or have PC loadings with absolute values greater than two standard deviations from the mean (points M−P). Significant (negative) rank order correlations exist between adult sex-bias size and fry epiallele variation in both PC1 ($p = 0.04$) and PC2 ($p < 0.0001$).

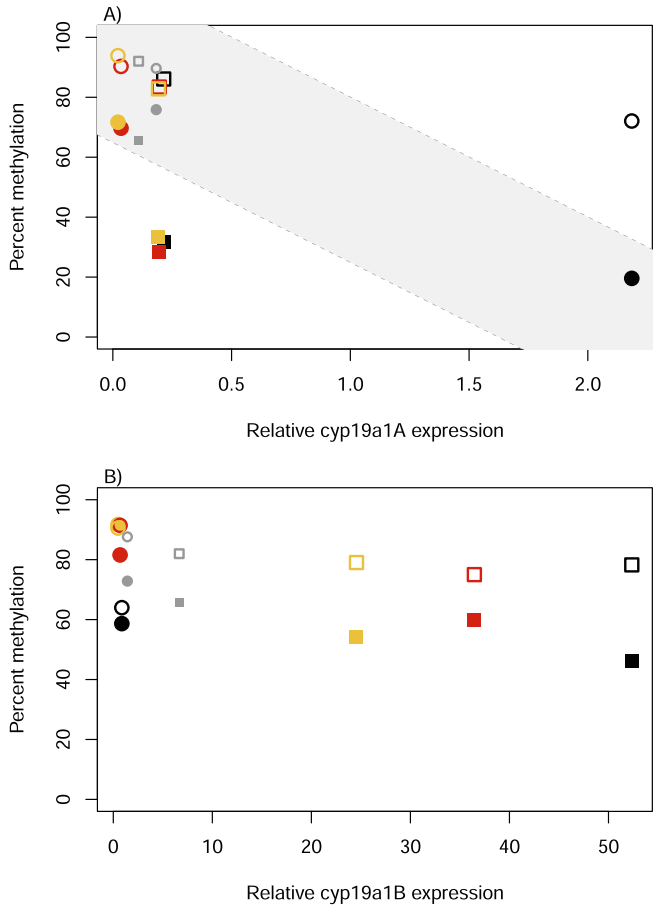

Fig. 9. Relationship between mean relative gene expression and mean percent methylation for cyp19A1 A-copy (A) and B-copy (B) including intergenic amplicons AI and BI (filled symbols) and proximal amplicons (open symbols) in both brain tissue (squares) and gonad tissue (circles) from adult females (black), male morphs (colored accordingly) and fry (grey). Note gene expression and methylation data derive from different individuals and relative gene expression of fry has been multiplied by a factor of 10 to include on the adult plot. Grey band in A denotes expected general relationship between gene expression and methylation state. AI in adult brain (filled squares) does not show the pattern predicted for a tissue-specificity and AP in female gonads does not show the pattern predicted for sex-specificity suggesting independent sex and tissue specific methylation patterns.

Less developmental work has addressed the timing of brain aromatase expression or methylation, and what work has been done shows no clear and simple pattern (Blazquez and Piferrer, 2004; Chang et al., 2005; Kallivretaki et al., 2007; Patil and Gunasekera, 2008; Trant et al., 2001; Vizziano-Cantonnet et al., 2011). Understanding the importance of brain aromatase to development and differentiation would seem to depend less on comparative surveys of the timing of expression and more on in-depth studies examining in a single species how the various aspects of differentiation are organized through this mechanism.

5. Conclusions

By sequencing both copies of the cyp19a1 gene and performing gene expression analysis and epigenetic analysis of two tissues in adult and fry, we have established *P. pulcher* as a system for the comparative study of mechanisms underlying environmental sex determination and alternative male morph development. In this species, the canonical teleost pattern of elevated expression of the A-copy in the female ovary and elevated expression of the B-copy in the brain was explained by methylation patterns most strongly for the A-copy in gonads according to our amplicon sequencing strategy. This is consistent with the relative density of CpGs upstream of these two genes. While we did not identify specific individual functional methylation sites, the different regions of the A-copy gene (intergenic vs. proximal) suggest independent tissue and sex-specific functions. Importantly, we showed that the discrete methylation patterns that differentiate male and female sex are among the most explanatory patterns for variation among individual fry, suggesting potential epigenetic marking of sex prior to differentiation and expression of the A-copy. A more detailed developmental time course and discrete dissection of gonads in fry will be helpful in addressing the epigenetic marks potentially introduced by environmental pH leading to male vs. female development or male morph expression.

CRediT authorship contribution statement

Rose M.H. Driscoll: Conceptualization, Methodology, Formal analysis, Investigation, Data curation. **Josh J. Faber-Hammond:** Software, Formal analysis, Visualization, Data curation. **Cynthia F. O'Rourke:** Methodology, Formal analysis, Visualization. **Peter L. Hurd:** Conceptualization, Formal analysis, Resources, Supervision. **Suzy C.P. Renn:** Conceptualization, Methodology, Validation, Visualization, Supervision.

Declaration of Competing Interest

The authors declare that they have no known competing financial interests or personal relationships that could have appeared to influence the work reported in this paper.

Acknowledgements

Members of the Hurd lab (Nicole Dittmann, McKenna Oleksuik, Nathan Brandwein, Brittany Hope, Kennedy Fjellner) assisted in animal husbandry and tissue collection. Avehi Singh assisted with molecular protocols. This work was funded by a Reed College Summer Research Fellowship to RMHD and SCPR, Reed College Presidential Fellowship to RMHD, Reed College Biology Undergraduate Research Proposal to RMHD, Reed College Initiative Grant to RMHD, NSERC Discovery Grant #RES0016396 to PLH and an NIH-NIGMS grant to SCPR #R15-DK116224-01.

Data Availability

Raw sequence data is available from GEO (#GSE135681)

Sequence data processing pipelines, as well as processed data and statistical analysis scripts that support the findings of the present study, are available on github (https://github.com/rose-driscoll/methylation-analysis).

Appendix A. Supplementary data

Supplementary data to this article can be found online at https://doi.org/10.1016/j.ygcen.2020.113538.

References

Aguiar, M., Masse, R., Gibbs, B.F., 2005. Regulation of cytochrome P450 by post-translational modification. Drug Metab. Rev. 37, 379–404.

Anastasiadi, D., Vandeputte, M., Sanchez-Baizan, N., Allal, F., Piferrer, F., 2018. Dynamic epimarks in sex-related genes predict gonad phenotype in the European sea bass, a fish with mixed genetic and environmental sex determination. Epigenetics 13, 988–1011.

Balthazart, J., Charlier, T.D., Cornil, C.A., Dickens, M.J., Harada, N., Konkle, A.T.M., Voigt, C., Ball, G.F., 2011. Sex differences in brain aromatase activity: genomic and non-genomic controls. Front. Endocrinol. 2, 34.

Baroiller, J.F., D'Cotta, H., Bezault, E., Wessels, S., Hoerstgen-Schwark, G., 2009a. Tilapia sex determination: where temperature and genetics meet. Comp. Biochem. Physiol.

A: Mol. Integr. Physiol. 153, 30–38.
Baroiller, J.F., D'Cotta, H., Saillant, E., 2009b. Environmental effects on fish sex determination and differentiation. Sex. Dev. 3, 118–135.
Bates, D., Machler, M., Bolker, B.M., Walker, S.C., 2015. Fitting linear mixed-effects models using lme4. J. Stat. Softw. 67, 1–48.
Bernstein, D.L., Kameswaran, V., Le Lay, J.E., Sheaffer, K.L., Kaestner, K.H., 2015. The BisPCR(2) method for targeted bisulfite sequencing. Epigenet. Chromatin 8.
Black, M.P., Balthazart, J., Baillien, M., Grober, M.S., 2005. Socially induced and rapid increases in aggression are inversely related to brain aromatase activity in a sex-changing fish, *Lythrypnus dalli*. Proc. R. Soc. B-Biol. Sci. 272, 2435–2440.
Blazquez, M., Gonzalez, A., Papadaki, M., Mylonas, C., Piferrer, F., 2008. Sex-related changes in estrogen receptors and aromatase gene expression and enzymatic activity during early development and sex differentiation in the European sea bass (*Dicentrarchus labrax*). Gen. Comp. Endocrinol. 158, 95–101.
Blazquez, M., Piferrer, F., 2004. Cloning, sequence analysis, tissue distribution, and sex-specific expression of the neural form of P450 aromatase in juvenile sea bass (*Dicentrarchus labrax*). Mol. Cell. Endocrinol. 219, 83–94.
Böhne, A., Heule, C., Boileau, N., Salzburger, W., 2013. Expression and sequence evolution of aromatase cyp19a1 and other sexual development genes in East African cichlid fishes. Mol. Biol. Evol. 30, 2268–2285.
Breton, T.S., DiMaggio, M.A., Sower, S.A., Berlinsky, D.L., 2015. Brain aromatase (cyp19a1b) and gonadotropin releasing hormone (gnrh2 and gnrh3) expression during reproductive development and sex change in black sea bass (*Centropristis striata*). Compar. Biochem. Physiol. a-Mol. Integr. Physiol. 181, 45–53.
Bulun, S.E., Sebastian, S., Takayama, K., Suzuki, T., Sasano, H., Shozu, M., 2003. The human CYP19 (aromatase P450) gene: update on physiologic roles and genomic organization of promoters. J. Steroid Biochem. Mol. Biol. 86, 219–224.
Callard, G., Schlinger, B., Pasmanik, M., 1990. Nonmammalian vertebrate models in studies of brain-steroid interactions. J. Exp. Zool. 4, 6–16.
Callard, G.V., Tchoudakova, A.V., Kishida, M., Wood, E., 2001. Differential tissue distribution, developmental programming, estrogen regulation and promoter characteristics of cyp19 genes in teleost fish. J. Steroid Biochem. Mol. Biol. 79, 305–314.
Cao, M.X., Duan, J.D., Cheng, N.N., Zhong, X.P., Wang, Z.Q., Hu, W., Zhao, H.B., 2012. Sexually dimorphic and ontogenetic expression of dmrt1, cyp19a1a and cyp19a1b in *Gobiocypris rarus*. Compar. Biochem. Physiol. A-Mol. Integr. Physiol. 162, 303–309.
Chang, X.T., Kobayashi, T., Senthilkumaran, B., Kobayashi-Kajura, H., Sudhakumari, C.C., Nagahama, Y., 2005. Two types of distribution aromatase with different encoding genes, tissue and developmental expression in Nile tilapia (*Oreochromis niloticus*). Gen. Comp. Endocrinol. 141, 101–115.
Chiang, E.F.L., Yan, Y.L., Guiguen, Y., Postlethwait, J., Chung, B.C., 2001. Two Cyp19 (P450 aromatase) genes on duplicated zebrafish chromosomes are expressed in ovary or brain. Mol. Biol. Evol. 18, 542–550.
Coveney, D., Shaw, G., Renfree, M.B., 2001. Estrogen-induced gonadal sex reversal in the tammar wallaby. Biol. Reprod. 65, 613–621.
Crews, D., Coomber, P., Baldwin, R., Azad, N., Gonzalez-Lima, F., 1996. Brain organization in a reptile lacking sex chromosomes: effects of gonadectomy and exogenous testosterone. Horm. Behav. 30, 474–486.
Cutting, A., Chue, J., Smith, C.A., 2013. Just how conserved is vertebrate sex determination? Dev. Dyn. 242, 380–387.
Czerwinski, M., Natarajan, A., Barske, L., Looger, L.L., Capel, B., 2016. A timecourse analysis of systemic and gonadal effects of temperature on sexual development of the red-eared slider turtle *Trachemys scripta elegans*. Dev. Biol. 420, 166–177.
D'Cotta, H., Fostier, A., Guiguen, Y., Govoroun, M., Baroiller, J.F., 2001. Aromatase plays a key role during normal and temperature-induced sex differentiation of Tilapia *Oreochromis niloticus*. Mol. Reprod. Dev. 59, 265–276.
Devlin, R.H., Nagahama, Y., 2002. Sex determination and sex differentiation in fish: an overview of genetic, physiological, and environmental influences. Aquaculture 208, 191–364.
Diotel, N., Le Page, Y., Mouriec, K., Tong, S.K., Pellegrini, E., Valliant, C., Anglade, I., Brion, F., Pakdel, F., Chung, B.C., Kah, O., 2010. Aromatase in the brain of teleost fish: Expression, regulation and putative functions. Front. Neuroendocrinol. 31, 172–192.
Dunham, I., Kundaje, A., Aldred, S., et al., 2012. An integrated encyclopedia of DNA elements in the human genome. Nature 489, 57–74.
Edgar, R.C., 2004. MUSCLE: multiple sequence alignment with high accuracy and high throughput. Nucleic Acids Res. 32, 1792–1797.
Edgar, R.C., 2010. Search and clustering orders of magnitude faster than BLAST. Bioinformatics 26, 2460–2461.
Ellison, A., Lopez, C.M.R., Moran, P., Breen, J., Swain, M., Megias, M., Hegarty, M., Wilkinson, M., Pawluk, R., Consuegra, S., 2015. Epigenetic regulation of sex ratios may explain natural variation in self-fertilization rates. Proc. R. Soc. B-Biol. Sci. 282, 20151900.
Eshed, Y., Feinberg, K., Poliak, S., Sabanay, H., Sarig-Nadir, O., Spiegel, I., Bermingham, J.R., Peles, E., 2005. Gliomedin mediates Schwann cell-axon interaction and the molecular assembly of the nodes of Ranvier. Neuron 47, 215–229.
Fan, Z., Zou, Y., Jiao, S., Tan, X., Wu, Z., Liang, D., Zhang, P., You, F., 2017. Significant association of cypl9a promoter methylation with environmental factors and gonadal differentiation in olive flounder *Paralichthys olivaceus*. Compar. Biochem. Physiol. A-Mol. Integr. Physiol. 208, 70–79.
Fergus, D.J., Bass, A.H., 2013. Localization and divergent profiles of estrogen receptors and aromatase in the vocal and auditory networks of a fish with alternative mating tactics. J. Compar. Neurol. 521, 2850–2869.
Flores, D., Tousignant, A., Crews, D., 1994. Incubation-temperature affects the behavior of adult leopard geckos (*Eublepharis-Macularius*). Physiol. Behav. 55, 1067–1072.
Forlano, P.M., Schlinger, B.A., Bass, A.H., 2006. Brain aromatase: new lessons from non-mammalian model systems. Front. Neuroendocrinol. 27, 247–274.
Fox, J., Weisberg, S., 2019. An R Companion to Applied Regression. Sage, Thousand Oaks, CA.
Galay-Burgos, M., Gealy, C., Navarro-Martin, L., Piferrer, F., Zanuy, S., Sweeney, G.E., 2006. Cloning of the promoter from the gonadal aromatase gene of the European sea bass and identification of single nucleotide polymorphisms. Compar. Biochem. Physiol. A-Mol. Integr. Physiol. 145, 47–53.
Golovine, K., Schwerin, M., Vanselow, J., 2003. Three different promoters control expression of the aromatase cytochrome P450 gene (Cyp19) in mouse gonads and brain. Biol. Reprod. 68, 978–984.
Goncalves, D., Teles, M., Alpedrinha, J., Oliveira, R.F., 2008. Brain and gonadal aromatase activity and steroid hormone levels in female and polymorphic males of the peacock blenny *Salaria pavo*. Horm. Behav. 54, 717–725.
González, A., Piferrer, F., 2002. Characterization of aromatase activity in the sea bass: effects of temperature and different catalytic properties of brain and ovarian homogenates and microsomes. J. Exp. Zool. 293, 500–510.
González., A, Piferrer, F., 2003. Aromatase activity in the European sea bass (Dicentrarchus labrax L.) brain. Distribution and changes in relation to age, sex, and the annual reproductive cycle. General and Comparative Endocrinology 2003 132, 223-230.
Gorelick, R., 2003. Evolution of dioecy and sex chromosomes via methylation driving Muller's ratchet. Biol. J. Linn. Soc. 80, 353–368.
Gross, M.R., 1996. Alternative reproductive strategies and tactics: diversity within sexes. Trends Ecol. Evol. 11, 92–98.
Heiligenberg, W., 1965. Colour polymorphism in the males of an African cichlid fish. Proceedings of the Zoological Society of London 146, 95-97.
Herpin, A., Schartl, M., 2015. Plasticity of gene-regulatory networks controlling sex determination: of masters, slaves, usual suspects, newcomers, and usurpators. EMBO Rep. 16, 1260–1274.
Heule, C., Göppert, C., Salzburger, W., Böhne, A., 2014a. Genetics and timing of sex determination in the East African cichlid fish *Astatotilapia burtoni*. BMC Genet. 15, 140.
Heule, C., Salzburger, W., Bohne, A., 2014b. Genetics of sexual development: an evolutionary playground for fish. Genetics 196, 579–591.
Ijiri, S., Kaneko, H., Kobayashi, T., Wang, D.-S., Sakai, F., Paul-Prasanth, B., Nakamura, M., Nagahama, Y., 2008. Sexual dimorphic expression of genes in gonads during early differentiation of a teleost fish, the Nile tilapia *Oreochromis niloticus*. Biol. Reprod. 78, 333–341.
Johnson, S.L., Brockmann, H.J., 2012. Alternative reproductive tactics in female horseshoe crabs. Behav. Ecol. 23, 999–1008.
Jones, P., 2012. Functions of DNA methylation: islands, start sites, gene bodies and beyond. Nat. Rev. Genet. 13, 484–492.
Kallivretaki, E., Eggen, R.I.L., Neuhauss, S.C.F., Kah, O., Segner, H., 2007. The zebrafish, brain-specific, aromatase cyp19a2 is neither expressed nor distributed in a sexually dimorphic manner during sexual differentiation. Dev. Dyn. 236, 3155–3166.
Kikuchi, K., Hamaguchi, S., 2013. Novel sex-determining genes in fish and sex chromosome evolution. Dev. Dyn. 242, 339–353.
Kitano, T., Takamune, K., Kobayashi, T., Nagahama, Y., Abe, S.I., 1999. Suppression of P450 aromatase gene expression in sex-reversed males produced by rearing genetically female larvae at a high water temperature during a period of sex differentiation in the Japanese flounder (*Paralichthys olivaceus*). J. Mol. Endocrinol. 23, 167–176.
Kobayashi, T., Kajiura-Kobayashi, H., Nagahama, Y., 2003. Induction of XY sex reversal by estrogen involves altered gene expression in a teleost, tilapia. Cytogenet. Genome Res. 101, 289–294.
Krueger, F., Andrews, S.R., 2011. Bismark: a flexible aligner and methylation caller for Bisulfite-Seq applications. Bioinformatics 27, 1571–1572.
Kuznetsova, A., Brockhoff, P.B., Christensen, R.H.B., 2019. Tests in linear mixed effects models. Package 3.1-0.
Kwon, J.Y., McAndrew, B.J., Penman, D.J., 2001. Cloning of brain aromatase gene and expression of brain and ovarian aromatase genes during sexual differentiation in genetic male and female Nile tilapia *Oreochromis niloticus*. Mol. Reprod. Dev. 59, 359–370.
Lance, V.A., 2009. Is regulation of aromatase expression in reptiles the key to understanding temperature-dependent sex determination? J. Exp. Zool. Part A-Ecol. Integr. Physiol. 311A, 314–322.
Langmead, B., Salzberg, S.L., 2012. Fast gapped-read alignment with Bowtie 2. Nat. Methods 9, 357–359.
Le Page, Y., Diotel, N., Vaillant, C., Pellegrini, E., Anglade, I., Merot, Y., Kah, O., 2010. Aromatase, brain sexualization and plasticity: the fish paradigm. Eur. J. Neurosci. 32, 2105–2115.
Lenth, R., Singmann, H., ., Love, J., Buerkner, P., Herveemmeans, M., 2019. emmeans: Estimated marginal means, aka least-squares means. https://cran.r-project.org/web/packages/emmeans.
Li, H., Handsaker, B., Wysoker, A., Fennell, T., Ruan, J., Homer, N., Marth, G., Abecasis, G., Durbin, R., 2009. The sequence alignment/Map format and SAMtools. Bioinformatics 25, 2078–2079.
Linke, H., Staeck, W., 1994. African Cichlids, I: Cichlids from West Africa. In: A Handbook for their Identification, Care and Breeding. Tetra Press, Melle Germany.
Maclusky, N.J., Naftolin, F., 1981. Sexual-differentiation of the central nervous-system. Science 211, 1294–1303.
Martin, E., Taborsky, M., 1997. Alternative male mating tactics in a cichlid, *Pelvicachromis pulcher*: A comparison of reproductive effort and success. Behav. Ecol. Sociobiol. 41, 311–319.
Masser, D.R., Stanford, D.R., Freeman, W.M., 2015. Targeted DNA methylation analysis by next-generation sequencing. Jove-J. Visual. Exp. 95, 52488.
Matsumoto, Y., Buemio, A., Chu, R., Vafaee, M., Crews, D., 2013. Epigenetic control of gonadal aromatase (cyp19a1) in temperature-dependent sex determination of red-

eared slider turtles. PLoS ONE 8, e63599.
McCarthy, M.M., Wright, C.L., Schwarz, J.M., 2009. New tricks by an old dogma: mechanisms of the Organizational Activational Hypothesis of steroid-mediated sexual differentiation of brain and behavior. Horm. Behav. 55, 655–665.
Moore, M.C., Hews, D.K., Knapp, R., 1998. Hormonal control and evolution of alternative male phenotypes: generalizations of models for sexual differentiation. Am. Zool. 38, 133–151.
Naftolin, F., Ryan, K.J., Davies, I.J., Reddy, V.V., Flores, F., Petro, Z., Kuhn, M., White, R.J., Takaoka, Y., Wolin, L., Wolin, L., 1975. The formation of estrogens by central neuroendocrine tissues. Recent Prog. Horm. Res. 31, 295–319.
Navarro-Martin, L., Vinas, J., Ribas, L., Diaz, N., Gutierrez, A., Di Croce, L., Piferrer, F., 2011. DNA methylation of the gonadal aromatase (cyp19a) promoter is involved in temperature-dependent sex ratio shifts in the European sea bass. PLoS Genet. 7, e1002447.
Nugent, B.M., McCarthy, M.M., 2011. Epigenetic underpinnings of developmental sex differences in the brain. Neuroendocrinology 93, 150–158.
Okubo, K., Takeuchi, A., Chaube, R., Paul-Prasanth, B., Kanda, S., Oka, Y., Nagahama, Y., 2011. Sex differences in aromatase gene expression in the medaka brain. J. Neuroendocrinol. 23, 412–423.
Parrott, B.B., Kohno, S., Cloy-McCoy, J.A., Guillette, L.J., 2014. Differential incubation temperatures result in dimorphic DNA methylation patterning of the SOX9 and aromatase promoters in gonads of alligator (*Alligator mississippiensis*) embryos. Biol. Reprod. 90, 1–11.
Partridge, C.G., MacManes, M.D., Knapp, R., Neff, B.D., 2016. Brain transcriptional profiles of male alternative reproductive tactics and females in bluegill sunfish. PLoS ONE 11, e0167509.
Pasmanik, M., Callard, G.V., 1985. Aromatase and 5-alpha-reductase in the teleost brain, spinal-cord, and pituitary-gland. Gen. Comp. Endocrinol. 60, 244–251.
Patil, J.G., Gunasekera, R.M., 2008. Tissue and sexually dimorphic expression of ovarian and brain aromatase mRNA in the Japanese medaka (*Oryzias latipes*): Implications for their preferential roles in ovarian and neural differentiation and development. Gen. Comp. Endocrinol. 158, 131–137.
Piferrer, F., 2013. Epigenetics of sex determination and gonadogenesis. Dev. Dyn. 242, 360–370.
Piferrer, F., Guiguen, Y., 2008. Fish Gonadogenesis. Part II: Molecular biology and genomics of sex differentiation. Rev. Fish. Sci. 16, 35–55.
Place, A.R., Lance, V.A., 2004. The temperature-dependent sex determination drama: same cast different stars., in: Valenzuela, N., Lance, V.A. (Eds.), Temperature-dependent sex determination in vertebrates. Smithsonian Books, Washington, pp. 99–110.
R-Core-Team, 2017. R: A Language and Environment for Statistical Computing, in: Computing, R.F.f.S. (Ed.) https://www.R-project.org. Vienna, Austria.
Ramsey, M., Shoemaker, C., Crews, D., 2007. Gonadal expression of Sf1 and aromatase during sex determination in the red-eared slider turtle (*Trachemys scripta*), a reptile with temperature-dependent sex determination. Differentiation 75, 978–991.
Reddon, A.R., Hurd, P.L., 2013. Water pH during early development influences sex ratio and male morph in a West African cichlid fish, *Pelvicachromis pulcher*. Zoology 116, 139–143.
Renn, S.C.P., Aubin-Horth, N., Hofmann, H.A., 2008. Fish and chips: functional genomics of social plasticity in an African cichlid fish. J. Exp. Biol. 211, 3041–3056.
Rhen, T., Crews, D., 1999. Embryonic temperature and gonadal sex organize male-typical sexual and aggressive behavior in a lizard with temperature-dependent sex determination. Endocrinology 140, 4501–4508.
Römer, U., Beisenherz, W., 1996. Environmental determination of sex in Apistogramma (Cichlidae) and two other freshwater fishes (Teleostei). J. Fish Biol. 48, 714–725.
Ru, W.X., Hua, L.S., Wei, Y.F., Li, W.Y., Cao, D.N., Ge, Y., Chen, H., Lan, X.Y., Gong, S.P., 2017. The effect of the Cyp19a1 gene methylation modification on temperature-dependent sex determination of Reeves' Turtle (*Mauremys reevesii*). Asian Herpetol. Res. 8, 213–220.
Rubin, D.A., 1985. Effect of pH on sex ratio in cichlids and a poecilliid (Teleostei). Copeia 1985, 233–235.
Schulz, R.W., de Franca, L.R., Lareyre, J.J., Legac, F., Chiarini-Garcia, H., Nobrega, R.H., Miura, T., 2010. Spermatogenesis in fish. Gen. Comp. Endocrinol. 165, 390–411.
Schunter, C., Vollmer, S.V., Macpherson, E., Pascual, M., 2014. Transcriptome analyses and differential gene expression in a non-model fish species with alternative mating tactics. BMC Genomics 15, 167.
Seaver, C.M.S., Hurd, P.L., 2017. Are there consistent behavioral differences between sexes and male color morphs in *Pelvicachromis pulcher*? Zoology 122, 115–125.
Ser, J.R., Roberts, R.B., Kocher, T.D., 2010. Multiple interacting loci control sex determination in Lake Malawi cichlid fish. Evolution 64, 486–501.
Shen, Z.G., Wang, H.P., 2014. Molecular players involved in temperature-dependent sex determination and sex differentiation in Teleost fish. Genet. Select. Evol. 46.
Siegfried, K.R., 2010. In search of determinants: gene expression during gonadal sex differentiation. J. Fish Biol. 76, 1879–1902.
Smith, C.A., Andrews, J.E., Sinclair, A.H., 1997. Gonadal sex differentiation in chicken embryos: expression of estrogen receptor and aromatase genes. J. Steroid Biochem. Mol. Biol. 62, 361.
Socorro, S., Martins, R.S., Deloffre, L., Mylonas, C.C., Canario, A.V.M., 2007. A cDNA for European sea bass (*Dicentrachus labrax*) 11 beta-hydroxylase: Gene expression during the thermosensitive period and gonadogenesis. Gen. Comp. Endocrinol. 150, 164–173.
Sudhakumari, C.C., Kobayashi, T., Kajiura-Kobayashi, H., Wang, D.S., Yoshikuni, M., Nagahama, Y., Senthilkumaran, B., 2005. Ontogenic expression patterns of several nuclear receptors and cytochrome P450 aromatases in brain and gonads of the Nile tilapia *Oreochromis niloticus* suggests their involvement in sex differentiation. Fish Physiol. Biochem. 31, 129–135.
Taborsky, M., Oliveira, R.F., Brockmann, H.J., 2008. The evolution of alternative reproductive tactics: Concepts and questions. In R. Oliveira, M. Taborsky, and H. Brockmann (Eds.), Alternative Reproductive Tactics: An Integrative Approach (pp. 1–22). Cambridge: Cambridge University Press.
Tanaka, M., Fukada, S., Matsuyama, M., Nagahama, Y., 1995. Structure and promoter analysis of the cytochrome-P-450 aromatase gene of the teleost fish, medaka (*Oryzias-Latipes*). J. Biochem. 117, 719–725.
Taylor, J.S., Braasch, I., Frickey, T., Meyer, A., Van de Peer, Y., 2003. Genome duplication, a trait shared by 22,000 species of ray-finned fish. Genome Res. 13, 382–390.
Tchoudakova, A., Callard, G.V., 1998. Identification of multiple CYP19 genes encoding different cytochrome P450 aromatase isozymes in brain and ovary. Endocrinology 139, 2179–2189.
Todd, E.V., Liu, H., Lamm, M.S., Thomas, J.T., Rutherford, K., Thompson, K.C., Godwin, J.R., Gemmell, N.J., 2018. Female mimicry by sneaker males has a transcriptomic signature in both the brain and the gonad in a sex-changing fish. Mol. Biol. Evol. 35, 225–241.
Trant, J.M., Gavasso, S., Ackers, J., Chung, B.C., Place, A.R., 2001. Developmental expression of cytochrome P450 aromatase genes (CYP19a and CYP19b) in zebrafish fry (*Danio rerio*). J. Exp. Zool. 290, 475–483.
Tsai, C.L., Chang, S.L., Wang, L.H., Chao, T.Y., 2003. Temperature influences the ontogenetic expression of aromatase and oestrogen receptor mRNA in the developing tilapia (*Oreochromis mossambicus*) brain. J. Neuroendocrinol. 15, 97–102.
Turecki, G., Meaney, M.J., 2016. Effects of the social environment and stress on glucocorticoid receptor gene methylation: a systematic review. Biol. Psychiatry 79, 87–96.
Valenzuela, N., Neuwald, J.L., Literman, R., 2013. Transcriptional evolution underlying vertebrate sexual development. Dev. Dyn. 242, 307–319.
Vizziano-Cantonnet, D., Anglade, I., Pellegrini, E., Gueguen, M.-M., Fostier, A., Guiguen, Y., Kah, O., 2011. Sexual dimorphism in the brain aromatase expression and activity, and in the central expression of other steroidogenic enzymes during the period of sex differentiation in monosex rainbow trout populations. Gen. Comp. Endocrinol. 170, 346–355.
Wang, Y.Y., Sun, L.X., Zhu, J.J., Zhao, Y., Wang, H., Liu, H.J., Ji, X.S., 2017. Epigenetic control of cyp19a1a expression is critical for high temperature induced Nile tilapia masculinization. J. Therm. Biol. 69, 76–84.
Wickham, H., 2007. Reshaping data with the reshape package. J. Stat. Softw. 21.
Wickham, H., François, R., Henry, L., Müller, K., 2018. dplyr: A Grammar of Data Manipulation. R package version 0.7.5. https://CRAN.R-project.org/package=dplyr.
Wu, G.-C., Chiu, P.-C., Lin, C.-J., Lyu, Y.-S., Lan, D.-S., Chang, C.-F., 2012. Testicular drmt1 Is involved in the sexual fate of the ovotestis in the protandrous black porgy. Biol. Reprod. 86, 1–11.
Yao, H.H., 2005. The pathway to femaleness: current knowledge on embryonic development of the ovary. Mol. Cell. Endocrinol. 230, 87–93.
Yoshida, K., Terai, Y., Mizoiri, S., Aibara, M., Nishihara, H., Watanabe, M., Kuroiwa, A., Hirai, H., Hirai, Y., Matsuda, Y., Okada, N., 2011. B chromosomes have a functional effect on female sex determination in Lake Victoria cichlid fishes. PLoS Genet. 7, e1002203.
Zhang, Y., Zhang, S., Liu, Z., Zhang, L., Zhang, W., 2013. Epigenetic modifications during sex change repress gonadotropin stimulation of cyp19a1a in a teleost ricefield eel (*Monopterus albus*). Endocrinology 154, 2881–2890.
Zhang, Y., Zhang, W.M., Yang, H.Y., Zhou, W.L., Hu, C.Q., Zhang, L.H., 2008. Two cytochrome P450 aromatase genes in the hermaphrodite ricefield eel *Monopterus albus*: mRNA expression during ovarian development and sex change. J. Endocrinol. 199, 317–331.